SINTEF
PROCEEDINGS
1

Selected papers from 10th International Conference on Computational Fluid Dynamics in the Oil & Gas, Metallurgical and Process Industries

# Progress in Applied CFD

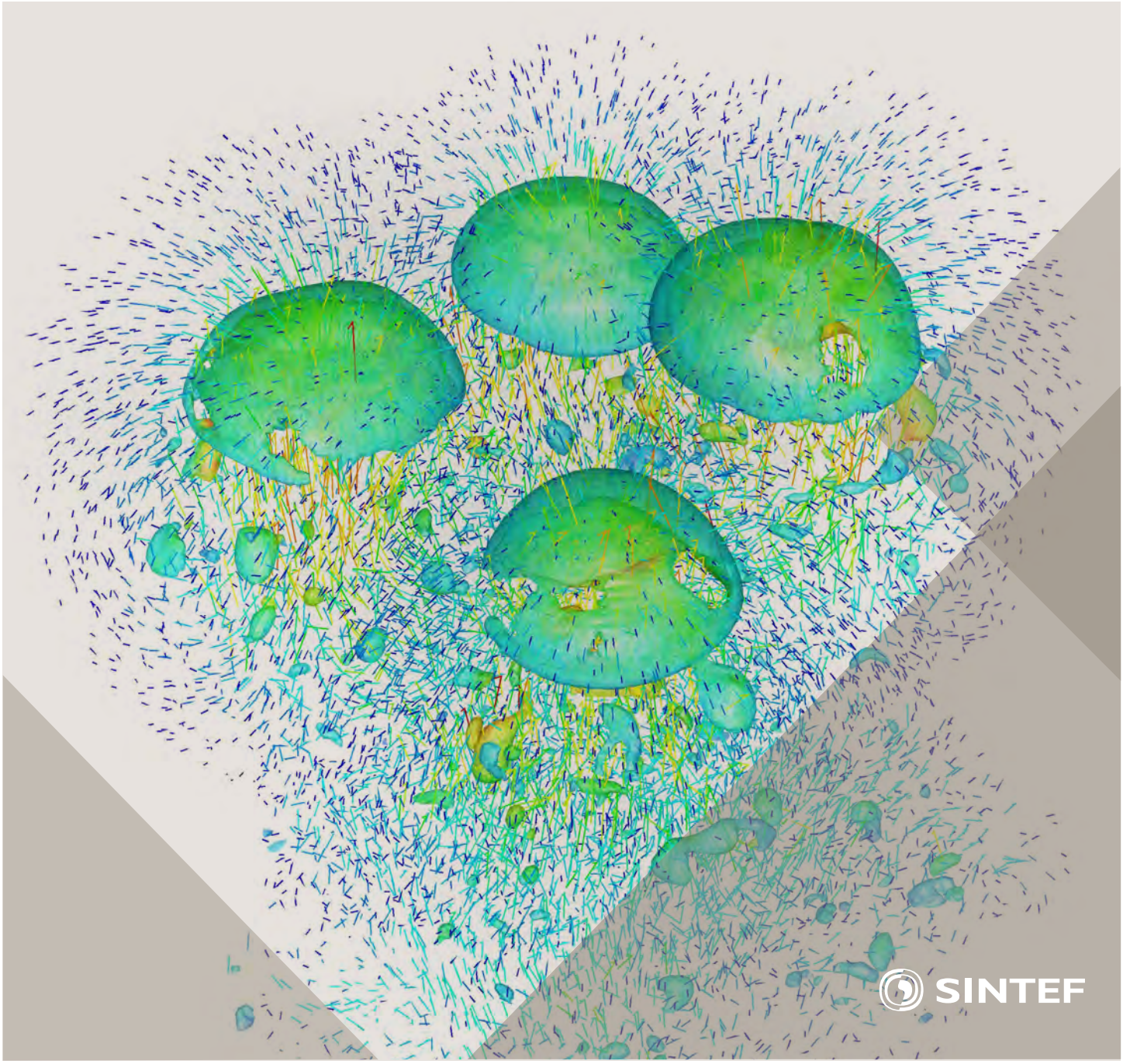

SINTEF Proceedings

Editors:
Jan Erik Olsen and Stein Tore Johansen

# Progress in Applied CFD

Selected papers from 10th International Conference on Computational Fluid Dynamics in the Oil & Gas, Metallurgical and Process Industries

SINTEF Academic Press

SINTEF Proceedings no 1
Editors: Jan Erik Olsen and Stein Tore Johansen
**Progress in Applied CFD**
Selected papers from 10th International Conference on Computational Fluid Dynamics in the Oil & Gas, Metallurgical and Process Industries

Key words:
CFD, Flow, Modelling

Cover, illustration: Rising bubbles by Schalk Cloete

ISSN 2387-4287 (printed)
ISSN 2387-4295 (online)
ISBN 978-82-536-1432-8 (printed)
ISBN 978-82-536-1433-5 (pdf)

60 copies printed by AIT AS e-dit
Content: 100 g munken polar
Cover: 240 g trucard



SINTEF Academic Press
Address: Forskningsveien 3 B
PO Box 124 Blindern
N-0314 OSLO
Tel: +47 22 96 55 55
Fax: +47 22 96 55 08

www.sintef.no/byggforsk
www.sintefbok.no

**SINTEF Proceedings**
SINTEF Proceedings is a serial publication for peer-reviewed conference proceedings on a variety of scientific topics.
The processes of peer-reviewing of papers published in SINTEF Proceedings are administered by the conference organizers and proceedings editors. Detailed procedures will vary according to custom and practice in each scientific community.

## PREFACE

This book contains selected papers from the 10th International Conference on Computational Fluid Dynamics in the Oil & Gas, Metallurgical and Process Industries. The conference was hosted by SINTEF in Trondheim in June 2014 and is also known as CFD2014 for short. The conference series was initiated by CSIRO and Phil Schwarz in 1997. So far the conference has been alternating between CSIRO in Melbourne and SINTEF in Trondheim. The conferences focus on the application of CFD in the oil and gas industries, metal production, mineral processing, power generation, chemicals and other process industries. The papers in the conference proceedings and this book demonstrate the current progress in applied CFD.

The conference papers undergo a review process involving two experts. Only papers accepted by the reviewers are presented in the conference proceedings. More than 100 papers were presented at the conference. Of these papers, 27 were chosen for this book and reviewed once more before being approved. These are well received papers fitting the scope of the book which has a slightly more focused scope than the conference. As many other good papers were presented at the conference, the interested reader is also encouraged to study the proceedings of the conference.

The organizing committee would like to thank everyone who has helped with paper review, those who promoted the conference and all authors who have submitted scientific contributions. We are also grateful for the support from the conference sponsors: FACE (the multiphase flow assurance centre), Total, ANSYS, CD-Adapco, Ascomp, Statoil and Elkem.

Stein Tore Johansen & Jan Erik Olsen

Organizing committee:

Conference chairman: Prof. Stein Tore Johansen
Conference coordinator: Dr. Jan Erik Olsen
Dr. Kristian Etienne Einarsrud
Dr. Shahriar Amini
Dr. Ernst Meese
Dr. Paal Skjetne
Dr. Martin Larsson
Dr. Peter Witt, CSIRO

Scientific committee:

J.A.M.Kuipers, TU Eindhoven
Olivier Simonin, IMFT/INP Toulouse
Akio Tomiyama, Kobe University
Sanjoy Banerjee, City College of New York
Phil Schwarz, CSIRO
Harald Laux, Osram
Josip Zoric, SINTEF
Jos Derksen, University of Aberdeen
Dieter Bothe, TU Darmstadt
Dmitry Eskin, Schlumberger
Djamel Lakehal, ASCOMP
Pär Jonsson, KTH
Ruben Shulkes, Statoil
Chris Thompson, Cranfield University
Jinghai Li, Chinese Academy of Science
Stefan Pirker, Johannes Kepler Univ.
Bernhard Müller, NTNU
Stein Tore Johansen, SINTEF
Markus Braun, ANSYS

## CONTENTS

# MODELLING OF THE FERROSILICON FURNACE: EFFECT OF BOUNDARY CONDITIONS AND SiO BURST

**Balram PANJWANI** [1]*, **Jan Erik OLSEN**[1†], **Bernd WITTGENS**[1‡]

[1]SINTEF Materials and Chemistry, 7465 Trondheim, NORWAY

*E-mail: balram.panjwani@sintef.no
† E-mail: jan.e.olsen@sintef.no
‡ E-mail: bernd.wittgens@sintef.no

## ABSTRACT

A by-product from the ferrosilicon process is process gas which escapes into the furnace hood were it reacts with air. The process gas mainly consists of CO with some SiO and moisture. Modeling the gas behavior inside the furnace hood is challenging due to the complex interaction between flow, reactions, radiation and turbulence. One of the issues is the selection of proper boundary conditions, especially, the boundary condition used for the charge surface through which the process gas is released, which strictly is neither a wall surface nor a mass flux boundary. Traditionally, this boundary condition is modeled as a mass flux boundary, without considering the effect of roughness due to uneven distribution of charge material. In present study, effect of accounting charge surface as a rough wall on the flow distribution is discussed. The results obtained from this study is compared with a simulation, where charge surface is modelled as a mass inlet boundary condition. Another issue is the boundary condition accounting for SiO burst. It is observed that process gas is frequently released in local bursts typically with a high concentration of SiO. This is believed to promote local hot spots, which favor $NO_X$ formation. Bursts of SiO are modeled and results show that both the strength of the burst and its location play a significant role in the $NO_X$ production.

**Keywords:** Ferrosilicon, Blowing, burst, SiO2 dust, Combustion, Charge surface.

## INTRODUCTION

Ferrosilicon is produced in submerged arc furnaces (SAF) where ore (silica) and carbon (coke, coal, etc.) are mixed inside a furnace. Both ore and carbon react when high voltage electric energy is supplied through electrodes, and this process is known as a reduction process. The reduction process produces alloys and an energy rich off-gas inside the reduction zone, which is beneath the charge surface and close to the electrode tip. The alloys, which are in liquid phase, sink to the bottom and this molten metal is collected through a tapping hole. The energy rich process gas rises upward from the reduction zone and escapes through the charge surface into a furnace hood. Simultaneously, air is sucked into the hood through various open areas on the furnace walls due to the pressure drop. The air and process gas reacts inside the furnace hood and produces an off-gas potentially containing harmful substances. In a ferrosilicon furnace, the process gas emerging from the charge surface mainly consists of CO with some SiO, water vapour, and volatiles. Reactions taking place between process gas and air in the furnace hood create temperature sufficiently high for formation of thermal $NO_X$. Release of process gas from the charge surface is non-uniform not only due to the transient and inhomogeneous reduction process but also due to inhomogeneous porosity distribution of charge material beneath the charge surface. Occasionally, the process gas (CO and SiO) bursts through the charge surface. These bursts mainly consist of high concentration of SiO. The reaction of SiO with air is highly exothermic resulting in local hot pockets inside the furnace hood, which subsequently leads to increase formation of $NO_X$. From industrial experience the strength of the jets or bursts and the amount of $NO_X$ formation are strongly correlated to each other. The high temperature bursts are triggered by avalanches in the charge. The charge avalanches causes outburst of large quantities of combustible gases, like CO/SiO, that rise from pockets of poorly carbonized charge material (Grådahl *et al.*, 2007). Blowing is another extreme situation, where SiO rich gas from around the electrode tip is released through a gas channel in the charge. Then large quantities of SiO are burnt in air to silica dust ($SiO_2$). The observed correlation between $NO_X$ and silica is also valid under blowing: blowing results in both high $NO_X$ and silica formation. Compared to the avalanche phenomenon, which is always short in duration, the blowing phenomenon can last much longer. A boundary condition accounting for SiO bursts is presented and its' impact on $NO_X$ Formation is also discussed.

Another challenge when modeling the combustion inside the furnace hoods is choice of boundary condition for the charge surface due to the non-uniform distribution of charge material (ore and carbon) on the surface. Traditionally, the charge surface is modeled as a mass flux boundary condition with no roughness effects accounted for. Alternatively, the charge surface can be modeled as a wall with roughness. However, a wall has no inherent inflow of fluid, which is required for the charge surface. While modeling the charge surface as

a wall boundary condition, a model that is valid for the range from smooth to fully rough walls is required. However, with the standard turbulence model to describe the near wall zone is not accurate and therefore special treatment is required closer to the inner wall regime. One of the common approaches is to use a wall function proposed by Launder and Spalding (Launder and Spalding, 1974). In this approach, the continuity and momentum equations along with the turbulence model equations are only solved in the outer region of the boundary layer. The inner region of the boundary layer is resolved with a predefined wall function. There have been many studies in the development of the wall function applicable for both smooth and rough walls (Jiménez, 2004). In this paper, a law of wall suitable for rough-wall surfaces is reviewed. While modeling the charge surface as a wall boundary condition the release of process gas from the charge surface need to be done explicitly. The most appropriate approach is to use source term for the mass, momentum, species and energy equations. These source terms will ensure that the correct amount of process gas with correct momentum and energy is released from the charge surface. Metal industries in Norway are committed toward the improvement of furnace operation, and their aim is to lower $NO_X$ levels and other pollutants and to achieve this, a better understanding of the flow phenomena inside the furnace hood and especially close to the charge surface is needed. Major aim of the present study is to gain more understanding of the flow phenomena taking place inside the furnace hood with help of CFD. A steady state CFD model is developed using the commercial software ANSYS FLUENT (ANSYS, 2011). The major objectives of the present research work is to address

1. How the surface roughness of the charge surface affects the flow distribution?
2. How do SiO bursts affect the temperature and $NO_X$ formation?
3. Does the location of burst have the impact on the $NO_X$ formation?

## CFD MODEL AND BOUNDARY CONDITIONS

A steady state CFD model solving for continuity, momentum, energy, species transport and radiation equations is developed using a general purpose CFD tool ANSYS FLUENT (ANSYS, 2011). The Radiation is modeled through Discrete Ordinance (DO) model, and the turbulence is modeled with RNG k-ε turbulence model, The near wall behavior is modelled with the standard wall functions. For rough walls appropriate roughness height and roughness constant are chosen. The process gas with a certain magnitude of velocity and temperature is escaped through the charge surface. It is rather easy to set the flow parameters of process gas at the charge surface using mass flux boundary condition, however, setting the process gas flow parameters at the charge surface with wall boundary condition is not very straightforward. FLUENT specific user defined functions (UDF) are employed to model the flow phenomena close to the charge surface. UDF for the source term in the continuity, momentum, energy and species transport equations were incorporated. The value of the source term was non-zero at the first grid cell of charge surface and zero for the rest of computational domain. The spatial discretization scheme was second order accurate. The pressure interpolation scheme was standard and the pressure gradient term was discretized using Green-Gauss cell based approach. The pressure velocity coupling was based on the SIMPLE algorithm.

## Combustion Model and Reaction Mechanism

In the present study Eddy Dissipation Concept model (EDC) was used for turbulence chemistry interaction (Magnussen and Hjertager, 1977). The EDC model is derived from turbulent energy cascade theory, where turbulent kinetic energy cascades from the larger eddies to smaller eddies. The cascading process continues until eddies are sufficiently small and they can't transfer energy further down. The EDC model assumes that the chemical reaction occurs on these smaller dissipative eddies, whose length and time scales are of the same order as the Kolmogorov length scale. Reaction within the fine eddies is assumed to occur as a constant pressure Perfectly Stirred Reactor (PSR) (GRAN and MAGNUSSEN, 1996a,b), where reactions proceed over the time scale, governed by the Arrhenius rates of Equation.

Table 1: Reduced reaction scheme with kinetic parameters in Kelvin, cal/mol, $cm^3$

| Reaction | Ar | N | Er |
|---|---|---|---|
| $2CO + O_2 \rightarrow 2CO_2$ | 2.24E+18 | 0.00 | 4776 |
| $2SiO + O_2 \rightarrow 2SiO2$ | 1.00E+18 | 0.00 | 0.24 |

The gas species accounted in the CFD model is CO, SiO and H2O originating from the furnace crater, $O_2$ and $N_2$ from surrounding air and $CO_2$ and $SiO_2$ which are products of the reactions. In the present study SiO2 is modeled as a gas phase, however heat of condensation from gas phase (SiO2) to solid phase (SiO2) is accounted in energy equation. Generally, there is an extensive reaction scheme governing the combustion process, accounting for detailed kinetics that lead to the larger CPU cost. Therefore, a simplified or reduced scheme shown in the Table 1 has been investigated. $NO_X$ formation is estimated using post processing approach available with FLUENT (ANSYS, 2011) but without considering the fluctuation in temperature and species.

### *Furnace Geometry and Computational Domain*

The modeled geometry is the pilot scale furnace designed and developed at SINTEF/NTNU. The pilot furnace is a kind of scaled version of the actual ferroalloys furnace; however, there are some noticeable differences. The pilot furnace has one electrode in the middle but the actual furnace consists of three electrodes. Furthermore, the height to diameter ratio of the pilot furnace is larger than height to diameter ratio of the actual furnace. Despite these differences, the processes such as reduction of ore and resulting process gas formation inside the pilot furnace are exactly

similar to the actual furnace. The pilot furnace can be operated with both AC and DC power supply. The furnace hood is connected to an off gas system, and equipment for monitoring composition and temperature of the gas is installed at the exhaust. A sketch of the furnace is shown in Figure 1. The original pilot furnace is asymmetric due to an offset in the exhaust, which makes impossible to investigate this geometry through 2D axis-symmetric approach, and therefore the geometry has to be modeled in 3D, which indeed results in higher CPU cost. 3D CFD validations of the pilot furnace have been performed under various conditions in previous work (Panjwani and Olsen, 2013).

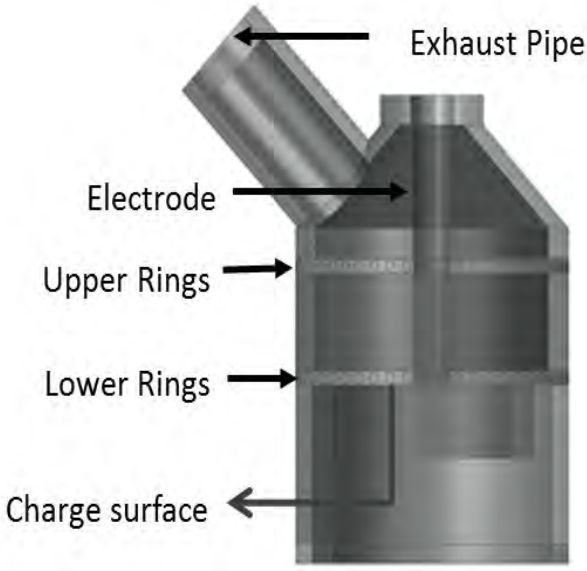


Figure 1: 3D schematic of the geometry

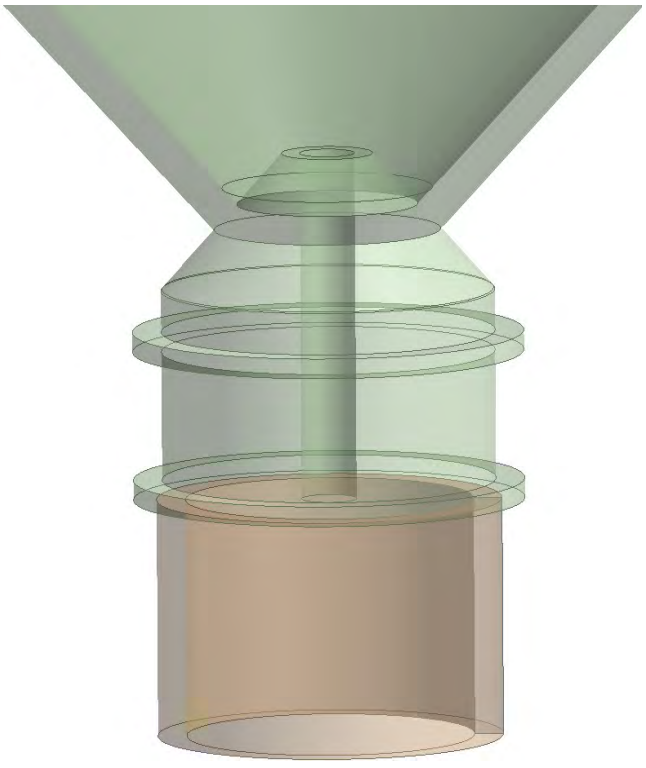

Figure 2: Schematic of the modified axis-symmetric geometry

In the present study, a modified pilot furnace, which is devised from original pilot furnace is proposed by modifying the exhaust pipe as shown in Figure 2.

This modification will allow 2D CFD simulations of the pilot furnace while preserving the underline physics of the ferrosilicon furnace. The furnace computational domain is divided into two domains, furnace domain (see Figure 2) and surrounding domain. The surrounding domain is a cylindrical volume around the furnace hood and it is a part of the computational domain. The surrounding domain is provided for an appropriate distribution of air flow through different openings on the furnace.

Most of the boundary conditions used for furnace modeling are difficult to measure, and are thus subject for qualified estimation based on experience. An important boundary condition is the amount of process gas escaping through the charge surface into the furnace hood. The metallurgical processes below the charge surface are responsible for process gas formation. These complex processes are not considered in the model. Therefore the amount of process gas is a priori unknown to the model. The only known parameters are the mass flow through the off-gas channel, offgas temperature and its composition. The mass flow and temperature of process gas escaping through the charge surface is thus estimated by tuning these values such that the measured mass flow and temperature in the off-gas channel is matched. Measuring the composition of off-gas and temperature at the off-gas channel is straightforward. For calculating the gas composition at the charge surface an elemental mass balance is performed. The composition of the process gas escaping through the charge surface is estimated from the measured composition in the off-gas channel and the composition of air from the surrounding.

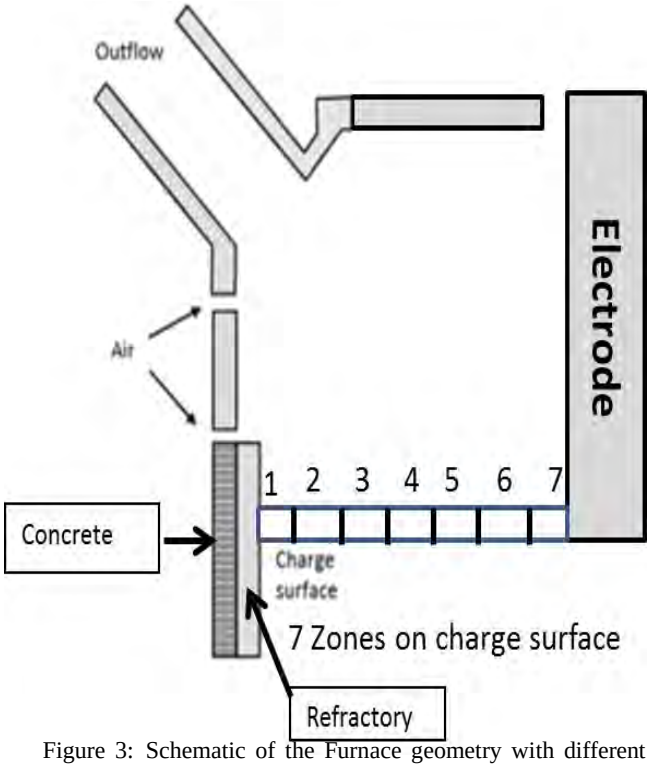


Figure 3: Schematic of the Furnace geometry with different zones and solid material

Since the process gas introduces molecules containing C and Si, the measured amounts of CO, $CO_2$ and $SiO_2$ in the off-gas will give the amount of CO and SiO in the process gas. Generally, a mass flux boundary is used at the charge surface.

The escaping of the process gas is non-uniform throughout the charge surface. Therefore the charge surface have been divided into seven zones (see Figure 3), which make easier to set different input values at different zones. The electrode is modeled as solid zone with a fixed power supply. On the wall boundaries depending on the type of the wall, a suitable boundary condition either convective or adiabatic is applied. The amount of air and its temperature being sucked into the furnace hood is supplied at the surrounding exterior surface through mass flux boundary condition. The mass flow rate through the surrounding was 1 kg/s and total amount of process gas was 0.08 kg/s. At the off-gas outlet, a pressure outlet boundary condition is employed. The specified outlet gauge pressure was 0 Pascal. The solid zones such as refractory, concrete and steel shown in Figure 2 are modeled explicitly.

CFD simulations were continued until all the residuals were below pre-specified values. In addition to that area averaged temperature at the offgas outlet surface was monitored. Our observation shows that even though the residuals for the governing equations were below the predefined value but the average temperature at outlet was not constant. Therefore, all the simulations were continued until both criteria were satisfied.

*Roughness Modeling*

The near-wall region consists of three main regimes: the laminar layer or linear sublayer, the buffer layer and the logarithmic layer. The laminar law holds in the linear sublayer, which is valid up to $y^+$=5. The logarithmic law holds in the log layer and it is valid from $y^+$=30 to $y^+$=500 - 1000. Nikuradse (Nikuradse, 1933) proposed the modification of the log law for rough surfaces by conducting extensive experiments on flow inside the rough pipe. According to Nikuradse (Nikuradse, 1933) the mean velocity distribution near rough walls has the same slope (1/κ) as smooth pipe but a different intercept. The law of the wall for mean velocity modified for roughness has following form (Cebeci and Bradshaw, 1977; Nikuradse, 1933):

$$\frac{U}{u^*} = \frac{1}{\kappa}\ln\left(\frac{\rho u^* y}{\mu}\right) + B - \Delta B \qquad (1)$$

$\Delta B$ depends, in general, on the type (uniform sand, rivets, threads, ribs, mesh-wire, etc.) and size of the roughness. For the fully rough regime, Cebeci and Bradshaw (Cebeci and Bradshaw, 1977) reported the following analytic fit to the sand-grain roughness data of Nikuradse (Nikuradse, 1933).

$$\Delta B = \frac{1}{\kappa}\ln f_r \qquad (2)$$

where $fr$ is a roughness function that quantifies the shift of the intercept due to roughness effects. There is no universal roughness function valid for all types of roughness. The roughness function is a function of $K^+ = \rho K_S u^*/\mu$, but takes different forms depending on the $K^+$ value. Where $K_S$ is the physical roughness height and $u^* = C^{1/4}k^{1/2}$. Based on the measurements three distinct regimes have been identified hydro dynamically smooth ( $K^+ \leq 2.25$), transitional ( $2.25 < K^+ \leq 90$) and fully rough ( $K^+ > 90$) According to the data, roughness effects are negligible in the hydro- dynamically smooth regime, but become increasingly important in the transitional regime, and take full effect in the fully rough regime. In FLUENT, the whole roughness regime is subdivided into the three regimes, and the formulas proposed by Cebeci and Bradshaw (Cebeci and Bradshaw, 1977) based on Nikuradse's (Nikuradse, 1933) data are adopted to compute $\Delta B$ for each regime.

## RESULTS AND DISCUSSIONS

In total eight steady state simulations were performed to understand the effect of burst on temperature and $NO_X$, appropriateness of boundary condition for charge surface, and effect of charge surface roughness on the mixing and rate of reaction closer to the charge surface. Before going into the further discussions on the effect of burst and boundary condition, we would like to discuss about velocity distribution inside the pilot furnace. Since, the velocity distribution inside the furnace hood obtained from CFD was quite similar to each other for all the simulation, therefore only one velocity vector is plotted for discussion. The velocity vector plot colored with O2 concentration for the pilot furnace is shown in Figure 4.

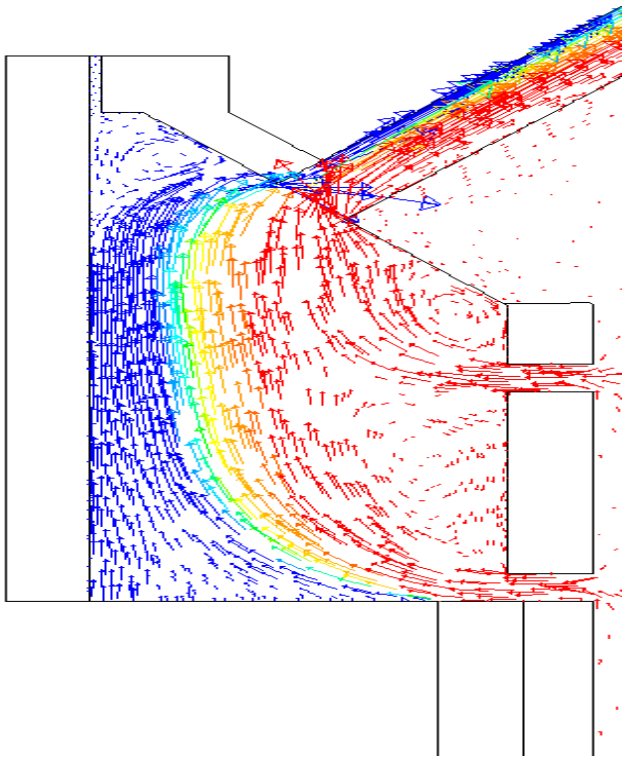

Figure 4: Vector plots for velocity distribution colored with $O_2$ mass fraction (max (red color)=0.23 and min (blue color)=0.0

It can be seen from vector plot that the air from the surrounding domain enters into the furnace through upper and lower rings/openings. The respective amount

of air entering through different openings on furnace depends mainly on the air mass flow rate through surroundings and the complex reaction processes taking place inside the furnace hood. The air entering through the lower ring/opening is parallel to the charge surface and it interacts with the process gas escaping through the charge surface. The rate of mixing depends on the air velocity magnitude and its direction and also on the roughness of the charge surface.

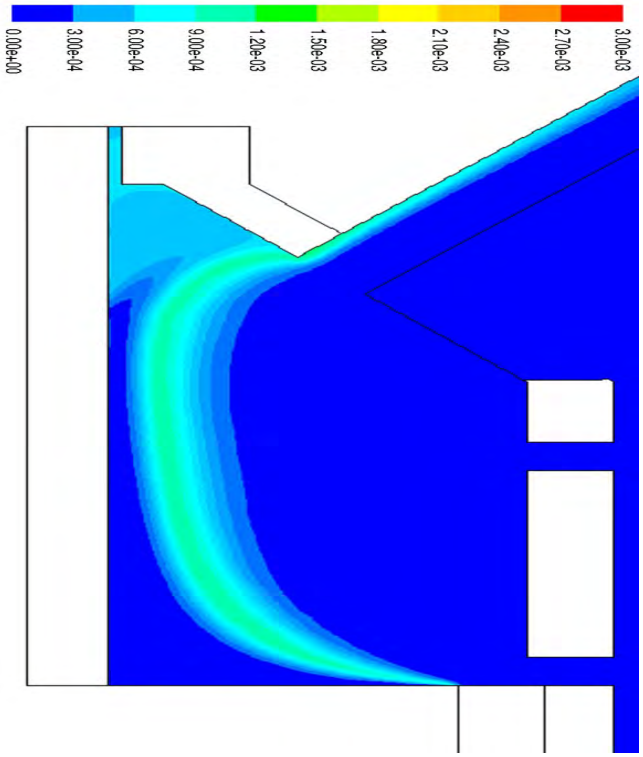


Figure 5: Contour plot of $SiO_2$ mass fraction (Case-1)

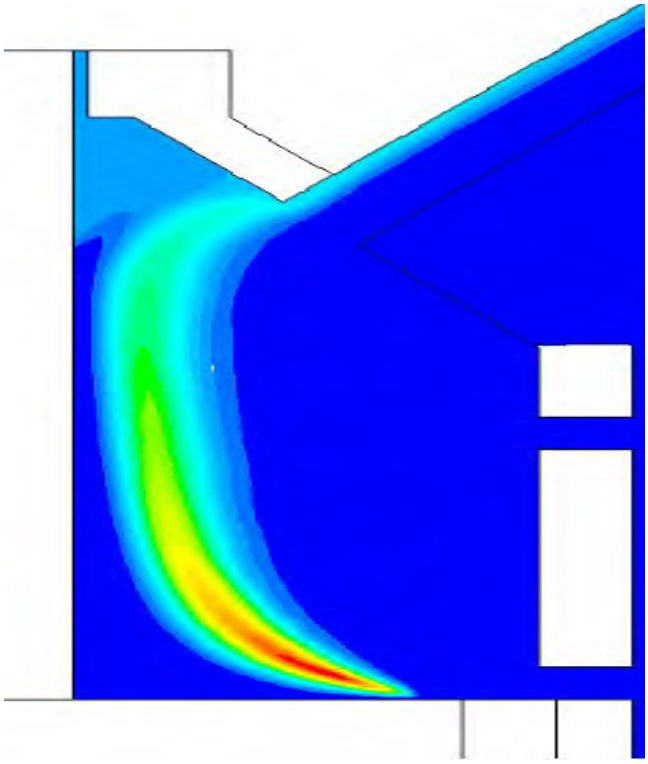

Figure 6: Contour plot of $SiO_2$ mass fraction (Case-2)

The flow around the roughened surface resembles as flow around the bluff bodies, and turbulence intensity behind the roughened surface depends on the roughness height and incoming velocity and its direction. Similarly, surface with higher roughness height will create large turbulence leading to the more mixing. It can also be seen (see Figure 4) that the air entering into furnace hood changes its direction from horizontal to the vertical due to the offgas location and buoyancy forces. Consequently, the air is not able to penetrate in the middle of the furnace hood.

*Process gas from Burst*

Occurrences of SiO burst have been observed in the real operation of ferrosilicon furnace. The burst causes a sudden release of SiO/CO jets through the charge surface. Influence of SiO burst on the temperature, $SiO_2$ species concentration and NOx formation is depicted through two CFD simulations. In Case-1, SiO was released uniformly throughout the charge surface and in Case-2, the same amount of SiO was released far from the electrode in the localized area on the charge surface. Formation rate of $SiO_2$ species concentration is much faster than the $CO_2$ gas formation rate due to the higher reaction rate of SiO with $O_2$ compare to the CO reaction rate with $O_2$.

Figure 5 and 6 show the $SiO_2$ distribution of Case-1 and Case-2 respectively. A large amount of $SiO_2$ concentration is clearly visible at the localized SiO release area (see Figure 6) when SiO is released in a concentrated way. However, $SiO_2$ concentration is diffused when SiO is released uniformly (see Figure 5). All the contour plots for $SiO_2$ distribution have been plotted on the same color bar and this color bar is shown in Figure 5.

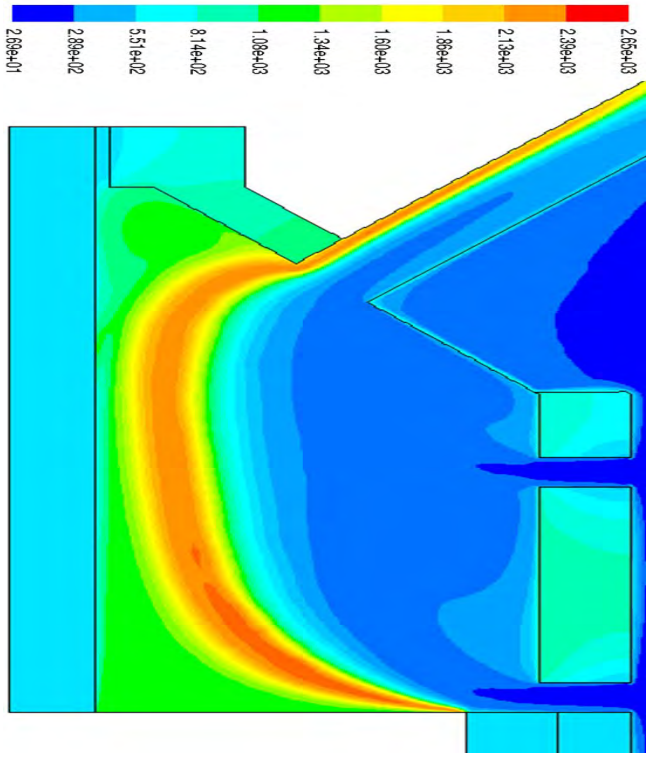


Figure 7: Contour plot of Temperature distribution ◦C (Case-1)

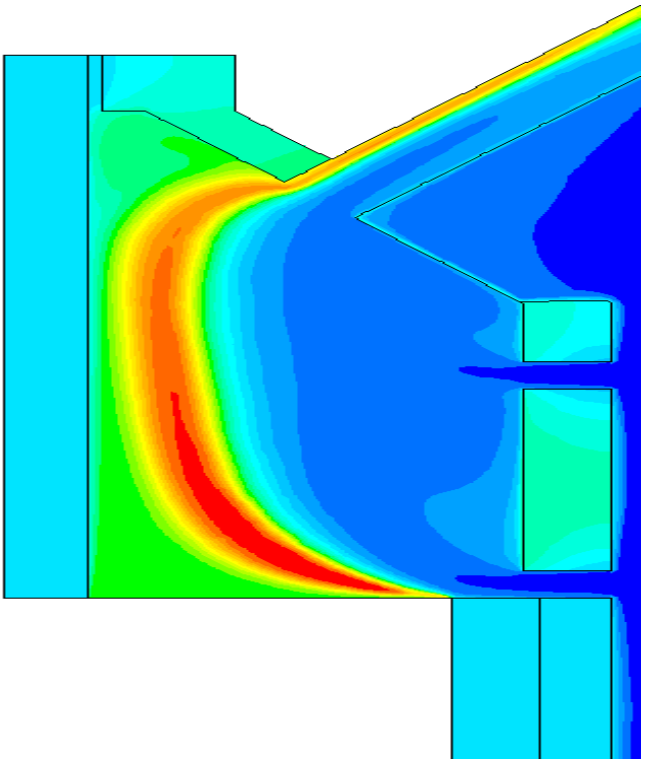

Figure 8: Contour plot of Temperature distribution ◦C (Case-2)

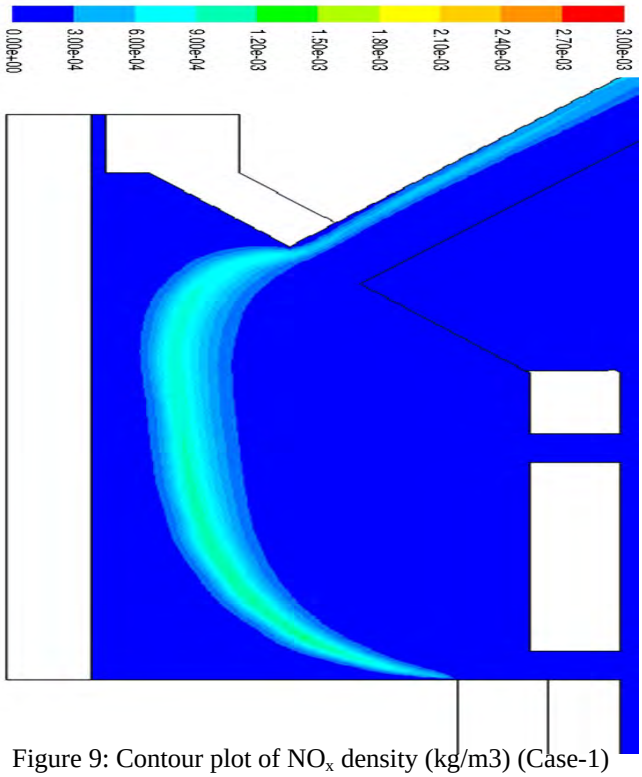


Figure 9: Contour plot of $NO_x$ density (kg/m3) (Case-1)

A common color bar for temperature, applicable for all the temperature contour plots, is shown in Figure 7. Similarly, a common color bar for NOx density, applicable for all the NOx density contour plots, is shown in Figure 9. Distribution of $NO_x$ density for Case-1 and Case-2 is shown in Figure 9 and 10 respectively. Total amount of $NO_x$ was 2.16 kg/hr when SiO was released uniformly from the charge surface, whereas the amount of $NO_x$ was 2.7 kg/hr when SiO was released in concentrated manner. It can be concluded from this study that the formation of burst leads to the higher $NO_x$ formation even though the average $SiO_2$ formation is same in both the operation. Normally, the formation of burst will be very irregular and it is very difficult to predict the location of the burst. However, the most likely location of the burst formation is close to the electrodes. One more CFD simulation, Case-3, was performed to understand the effect of location of SiO burst on flow behavior. In Case-3, it was assumed that the SiO burst occur close to the electrode. It has been observed from velocity vector plot the air does not penetrate in the middle of furnace hood (see Figure 4) and there is not enough air close to the electrode. Therefore, in a limited amount of air supply there is less possibility of the SiO reaction near to the electrode and closer to the charge surface. In this situation most of the SiO reacts above the charge surface but closer to the exhaust pipe, where concentration of air is higher (see Figure 11).

It can be concluded from the results obtained from Case-2 and Case-3 that not only the location of burst but also the availability of air affects the $NO_x$ formation. In present study only the reaction of SiO with $O_2$ is considered. It is not very clear whether SiO reacts with other species such as $H_2O$, CO and $CO_2$.

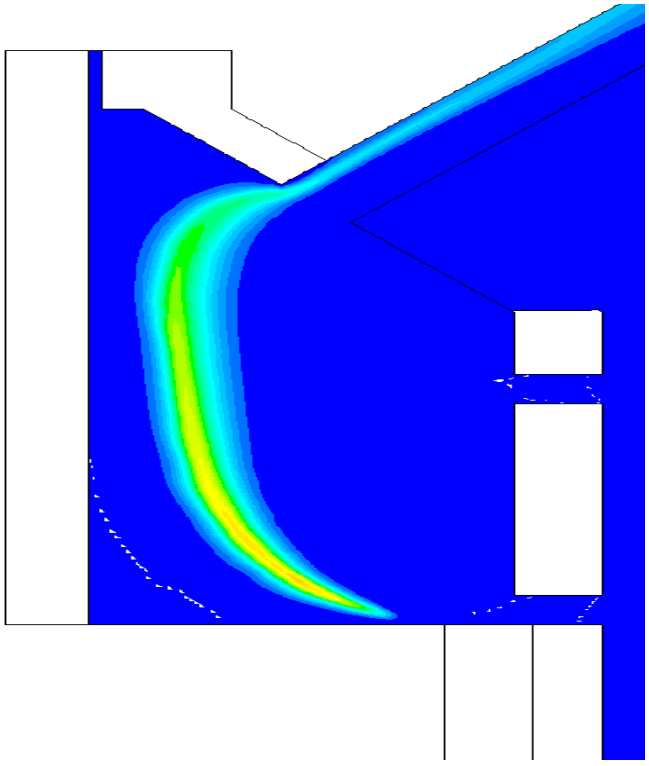

Figure 10: Contour plot of $NO_x$ density (kg/m3) (Case-2)

Previous measurements have shown that the $SiO_2$ species concentration correlate well with the NOx formation. Increase in the $SiO_2$ concentration leads to increase in the $NO_x$. In order to understand this effect one more CFD simulation, Case-4, is carried out. The Case-4 is similar to the Case-2, except SiO release rate

is five times larger as compared to the Case-2. The simulation parameters of Case-4 were the same as Case-2. Figure 12 shows the $SiO_2$ mass fraction of Case-4, it can be seen that an increase in SiO concentration leads to the increased concentration of $SiO_2$. This increase in $SiO_2$ concentration also leads to the increase in temperature and subsequent $NO_x$ formation as shown in Figure 13. The studies shows that total amount of $NO_x$ increases up to 6.5 kg/hr from 2.7 kg/hr by increasing the SiO mass fraction by five times.

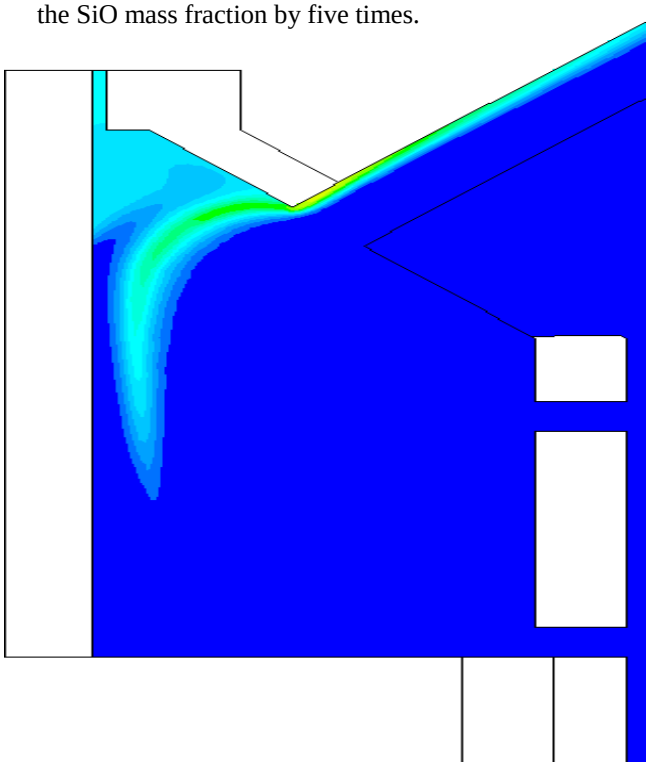

Figure 11: Contour plot of $SiO_2$ mass fraction (Case-3)

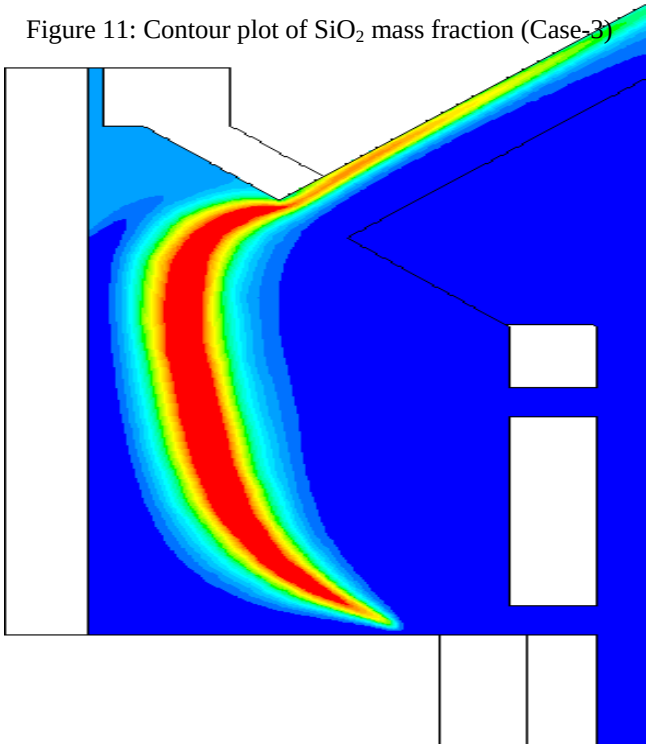

*Figure 12: Contour plot of $SiO_2$ mass fraction (Case-4)*

*Effect of boundary condition*

Two CFD simulations: Case-5 and Case-6 were carried out, Case-5 corresponds to the situation where mass flux boundary condition was applied on the charge surface, whereas Case-6 refers to the situation where wall boundary condition was applied on the charge surface. Otherwise, all other boundary conditions, chosen models and numerical schemes are same in both the cases.

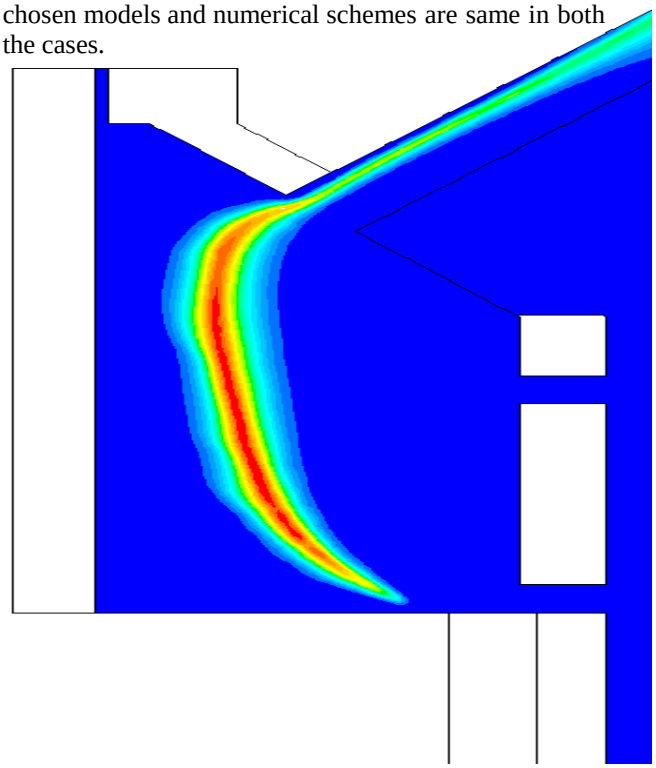

Figure 13: Contour plot of $NO_x$ density ($kg/m^3$) (Case-4)

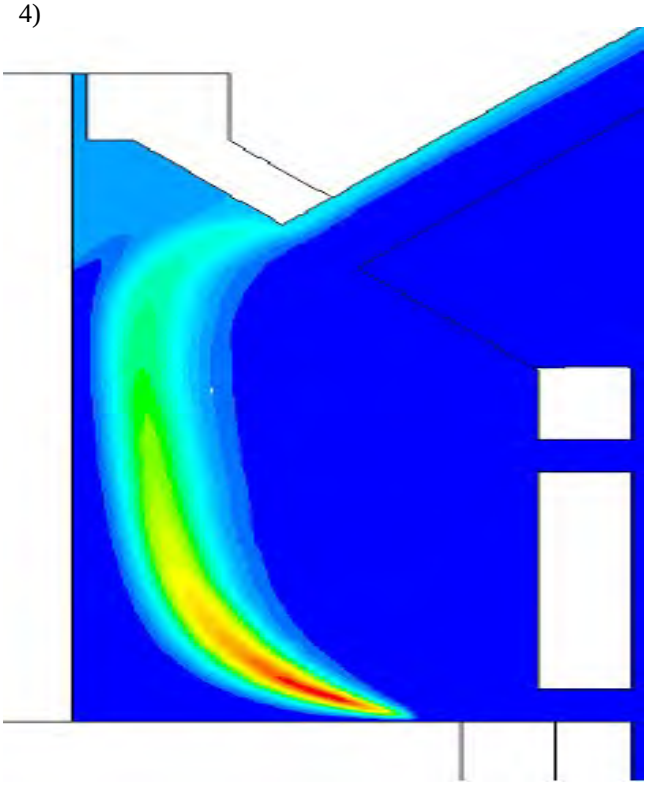

Figure 14: Contour plot of $SiO_2$ mass fraction (Case-5)

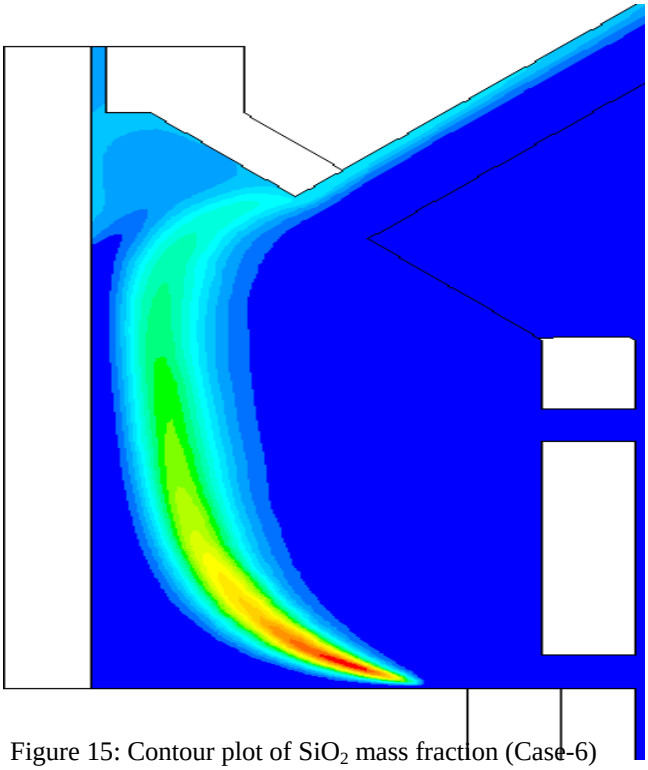

Figure 15: Contour plot of $SiO_2$ mass fraction (Case-6)

In Case-6, the roughness effects are not considered because an aim of this simulation (Case-6) was to find the appropriateness of the wall boundary condition for the charge surface in a place of mass flux boundary condition.

Figure 14 and 15 shows the $SiO_2$ mass fraction of Case- 5 and Case-6 respectively. It can be seen that there is not any significant difference between $SiO_2$ distribution obtained from both simulations. Although the results obtained from both the boundary conditions are similar, applicability of the wall boundary condition poses a challenge. In addition, one of the biggest challenges is to calculate the source terms for momentum and energy equation from the species mass source.

One of the biggest advantages offered by mass flux boundary is that all the flow variables of the charge surface can be set very conveniently. As it is mentioned that a main purpose of performing simulation with wall boundary condition is to account for the surface roughness of the charge surface. The wall roughness influences the mixing between process gas emerging from the charge surface and incoming air flow from lower opening. In ferrosilicon furnace, at what extent roughness affects the mixing is not very clear. Now, there is an open question whether accounting roughness, which improves physics close to the wall but introduces complexity in modeling the charge surface, overweight the simplification offered by the mass flux boundary condition. To answer this question two more CFD simulation, with and without charge surface roughness, are performed. FLUENT specific wall roughness model was chosen. The roughness height $K_s$ was 4 mm and roughness constant $C_s$ was 0.5. Present study showed that there was not any significant differences between the flow field of smooth and rough charge surface cases while examining the contour plots for both cases. To illustrate this, a radial velocity distribution for both cases is plotted and shown in Figure 16. Difference in velocity can hardly be noticed in the radial velocity profiles. A similar behavior was also observed in the axial velocity profile (not shown here). To illustrate the effect of the roughness on skin friction, the skin friction coefficients of the charge surface wall is plotted for both rough and smooth cases (see Figure 17).

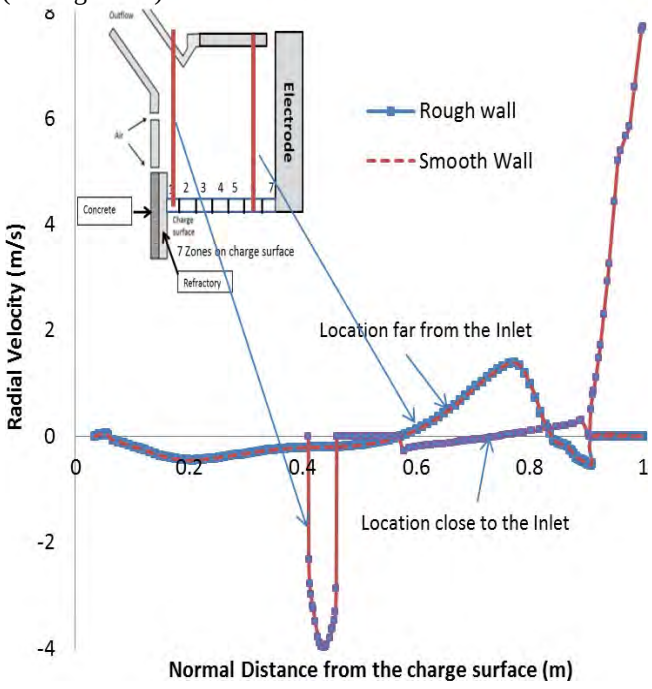


Figure 16: Radial Velocity profiles for smooth and rough charge surface

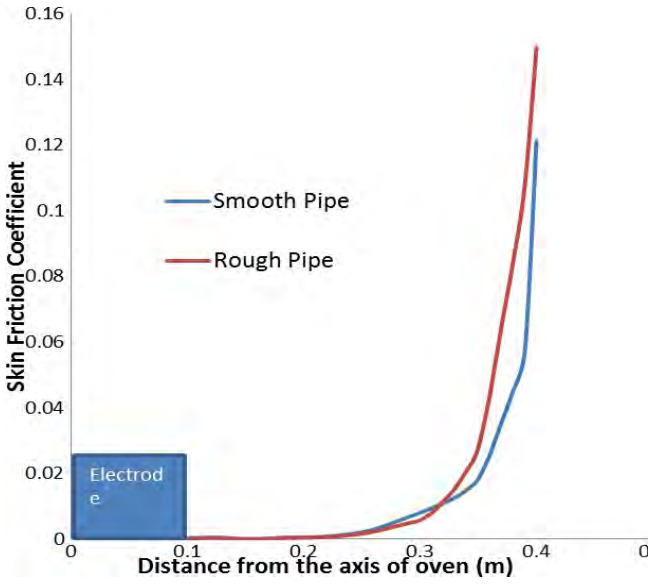


Figure 17: Skin friction coefficients for smooth and rough charge surface

A noticeable difference in the skin friction coefficient can be seen at the location close to the inlet, however far from the inlet the skin friction coefficient is negligible. The reason for this behavior can be understood by carefully examining the velocity vectors (see Figure 4). It can be seen that the incoming air from

the surrounding domain is parallel to the charge surface. Therefore higher value of skin friction coefficient is observed at the location close to the inlet (far from the electrode), However, due to the upward pressure gradients inside the furnace the direction of flow becomes normal to the charge surface at a location slightly far from opening and this leads to reduction in skin friction coefficient. From present study, it is very difficult to identify the role of charge surface roughness on turbulent mixing and reaction. Furthermore, applicability of the wall roughness models is questionable under strong lateral pressure gradient cases. The impact of wall roughness on mixing and subsequent reaction can be well understood through an explicit modeling of charge surface roughness.

## CONCLUSIONS

A steady state CFD model solving for governing equation is developed using ANSYS FLUENT. Two approaches: wall boundary condition and mass flux boundary condition for modeling the charge surface is presented. Studies showed that both approaches give a similar result but using a wall boundary condition is a challenge. Furthermore, simplified approaches for modeling the SiO jets have been discussed in this study. Study showed that the concentrated SiO generates local zones of higher temperature, which are responsible for NOx formation. In addition to that, location of the SiO jets and local distribution of air supply play a major role in the NOx formation.

## REFERENCES

ANSYS (2011). ANSYS FLUENT Theory Guide, V 13.

CEBECI, T. and BRADSHAW, P. (1977). *Momentum Transfer in Boundary Layers, ISBN:978-0070103009*. Hemisphere-McGraw-Hill, New York.

GRAN, I.R. and MAGNUSSEN, B.F. (1996a). "A numerical study of a bluff-body stabilized diffusion flame. part 1. influence of turbulence modeling and boundary conditions". *Combustion Science and Technology*, **119(1-6)**, 171–190.

GRAN, I.R. and MAGNUSSEN, B.F. (1996b). "A numerical study of a bluff-body stabilized diffusion flame. part 2. influence of combustion modeling and finite-rate chemistry". *Combustion Science and Technology*, **119(1-6)**, 191–217.

GRåDAHL, S. *et al.* (2007). "Reduction of emissions from ferroalloy furnaces". *INFACON XI, India*, 479–488.

JIMéNEZ, J. (2004). "Turbulent flows over rough walls".*Annual Review of Fluid Mechanics*, **36(1)**, 173–196.

LAUNDER, B. and SPALDING, D. (1974). "The numerical computation of turbulent flows". *Computer Methods in Applied Mechanics and Engineering*, **3(2)**, 269 – 289.

MAGNUSSEN, B. and HJERTAGER, B. (1977). "On mathematical modeling of turbulent combustion with special emphasis on soot formation and combustion". *Symposium (International) on Combustion*, **16(1)**, 719 – 729.

NIKURADSE, J. (1933). "Laws of flow in rough pipe" Tech. Rep. TECHNICAL MEMORANDUM1292/Forschung Arb. Ing.-Wes. No. 361.

PANJWANI, B. and OLSEN, J.E. (2013). "Combustionand mechanisms for $NO_x$ formation in ferrosilicon electric arc furnaces". *European Combustion Meeting, ECM, Lund University, Sweden*.